Synthesis and Characterization of an Amphiphilic Hyperbranched Poly(amine-Ester)-*co*-D,L-lactide (HPAE-*co*-PLA) Copolymers and Their Nanoparticles for Protein Drug Delivery

Ming Jiang,[1,2] Yan Wu,[2] Yong He,[1] Jun Nie[1]

[1]*State Key Laboratory of Chemical Resource Engineering Key Lab of Beijing City on Preparation and Processing of Novel Polymer Materials, Beijing University of Chemical Technology, Beijing 100029, People's Republic of China*
[2]*National Center for Nanoscience and Technology, Beijing 100190, People's Republic of China*

Received 12 November 2008; accepted 27 November 2009
DOI 10.1002/app.31868
Published online 26 March 2010 in Wiley InterScience (www.interscience.wiley.com).

ABSTRACT: A series of hyperbranched poly(amine-ester)-*co*-D,L-lactide (HPAE-*co*-PLA) copolymer were synthesized by ring-opening polymerization of D,L-lactide with $Sn(Oct)_2$ as catalyst to a fourth generation branched poly(amine-ester) (HPAE-OHs4). The chemical structures of copolymers were determined by FTIR, ^{1}H-NMR, ^{13}C-NMR, and TGA. Double emulsion (DE) and nanoprecipitation (NP) method were used to fabricate the nanoparticles of these copolymers encapsulating bovine serum albumin (BSA) as a model. DSC thermo-grams indicated that the nanoparticles with BSA kept stable below 40°C. Different factors which influence on particular size and encapsulation efficiency (EE) were investigated. Their EE to BSA could reach 97.8% at an available condition. *In vitro* release behavior of NPs showed a continuous release after a burst release. The stability maintenance of BSA in the nanoparticle release *in vitro* was also measured via circular dichroism and fluorescence spectrometry. The results showed that the copolymer nanoparticles have a promising potential in protein delivery system. J Appl Polym Sci 117: 1156–1167, 2010

Key words: hyperbranched poly(amine-ester); poly(lactide); amphiphilic copolymer; bovine serum albumin; protein delivery system

INTRODUCTION

The physico–chemical and biological properties of protein and peptide drugs (PPD) are different from those of conventional ones, such as molecular size, biological half-life, conformational stability, physico–chemical stability, solubility, oral bioavailability, dose requirement, and administration, etc. Therefore, design and manufacturing of PPD delivery systems have been a challenging area of research. So far, some of conventional colloidal drug delivery systems, such as liposomes and nanoparticles (NPs), have been developed and tested for PPD. Polymeric micelles prepared from amphiphilic copolymers as a carrier system for delivery of drugs has gained increasing interest. Polymeric micelles are conjugated or interacted with a therapeutic agent of interest within their polymeric matrix or onto the surface, and the NPs were easily adsorbed by protein and phagocytosed by cells of the reticuloeddothelial system (RES).[1–7] Polymeric micelles present numerous advantages, such as reduced side effects of anticancer drugs and selective targeting, it also allows for controlling the release pattern of drug and sustaining drug levels for a long time by appropriately selecting the polymeric carrier.

Dendritic polymers including dendrimers and hyperbranched polymers have a highly branched structure, intramolecular voids, small rheological volumes, lower viscosity in solution, providing a high density of functional groups at the periphery.[8–10] It is also suitable for a wide range of biomedical applications including drug delivery, detoxication, microarray systems and catalysis.[11–13] Dendrimers which may have more defined and ordered branching structure have to be obtained step by step with time-consuming and expensive

Correspondence to: Y. Wu (wuyan66@eyou.com).
Contract grant sponsor: National High Technology Research and Development Program of China; contract grant number: 2006AA03Z321.
Contract grant sponsor: Fundamental research of the Chinese academy of sciences; contract grant number: KJCX2-YW-M02.
Contract grant sponsor: State Key Development Program for Basic Research of China; contract grant numbers: 2009CB930200, 2010CB934004.

synthetic and purification procedures.[14,15] In comparison, hyperbranched polymer, which has similar figuration as dendrimer and was synthesized much easier than dendrimer, may be a new type of potential application for the drug delivery system.[16,17] Hyperbranched polymers contain numerous end-groups in their molecular structures and the characteristics of these terminal groups have a great influence on the properties of resulting hyperbranched polymers. Therefore, modification of the number and type of end-groups is a powerful tool to tailor the properties of hyperbranched polymers.[18]

In this article, we synthesized the fourth generation of hyperbranched poly(amine-ester) (HPAE-OHs) with well-defined primary structure in pseudo-one-step process.[19,20] The polymers contain repeating internal tertiary amine-linkage and abundant surface hydroxyl groups that enable further modification. The polymers were then designed to introduce the PLA by modification of the surface hydroxyl groups of the product. The copolymers were characterized on the basis of ^{1}H-NMR, ^{13}C-NMR, and FTIR measurements. Bovine serum albumin is similar to serum albumin of in the abound presence of human body. Bovine serum albumin (BSA), which is often chosen as a model protein for encapsulation studies in the nanoparticles made of PLGA and PEG–PLA due to its well-known physico–chemical properties and low cost,[21] was encapsulated within nanoparticles made of HPAE-*co*-PLA with the double emulsion (DE) and nanoprecipitation (NP) method. The morphological examination of nanoparticles was performed using a transmission electron microscope (TEM) for morphology analysis, encapsulation efficiency, release profiles and stability of BSA released from the NPs were also investigated.

EXPERIMENTAL

Materials

1,1,1-trimethylol propane of reagent grade, methyl acrylate purified by vacuum distillation and diethanolamine were purchased from National Medicines chemical Reagent (China), titanium tetraisopropoxide ($Ti(OiPr)_4$), benzoic anhydride and imidazole were purchased from Beijing Reagent Factory, (China), D,L-lactide (DLLA) was obtained from (Alfa Aesar, America), $Sn(Oct)_2$ was purchased from Sigma, Poly(vinyl alcohol) (PVA) was purchased from Guangdong, XILONG Chemical Industry (China), BSA (M_w = 66 kDa) was purchased from Sigma (St. Louis, MO). BCA protein assay kit was purchased from Beyotime Institute of Biotechnology (China). All other reagents and solvents were of analytical grade.

Synthesis and characterizations of HPAE-*co*-PLA copolymer

Synthesis HPAE-OHs

HPAE-OHs with surface hydroxyl groups was prepared according to the previous article[19] with few modifications. The synthesis route is shown in Scheme 1(a). HPAE-OHs were synthesized through a pseudo-one-step process by alcoholysis at 120°C using 1,1,1-trimethylol propane (as a molecular core) and *N,N*-diethylol-3-amine methylpropionate (as an AB_2monomer) with Ti $(OiPr)_4$ as the catalyst. The generation of HPAE-OHs was increased by repeatedly adding *N,N*-diethylol-3-amine methylpropionate monomer to the former generation product. The fourth-generation HPAE-OHs4 was obtained by repeating the process three times. The product was dissolved in 10 mL ethanol, and the $Ti(OiPr)_4$ produced the precipitate in ethanol. Then, the $Ti(OiPr)_4$ was removed by filtration. Finally the ethanol was evaporated and the product were dried at 40°C in a vacuum oven and stored for further utilization. *N,N*-diethylol-3-amine methylpropionate was prepared by using methyl acrylate and diethanolamine, the feed molar ratio is 1.5 : 1. After the Michael Reaction, excess methyl acrylate and methanol was removed by vacuum distillation. To minimize the side reactions between the AB_2 monomer, the choice of effectively-available transesterification catalysts which show the best compromise between chemioselecivity and activity has attracted growing attention in chemical reactions. It showed that titanates and zirconates were the most interesting catalysts.[22] Because of above reasons, *p*-methylbenzene sulfonic acid (*p*-TsOH) was replaced by $Ti(OiPr)_4$. The final products of HPAE-OHs4 have good solubility in water, ethanol and *N,N*-Dimethylformamide (DMF).

Synthesis of HPAE-*co*-PLA copolymer

HPAE-*co*-PLA copolymer [in the molar ratio of 3 : 1–10 : 1 (DLLA/ HPAE–OHs4)] was synthesized utilizing a ring-opening polymerization procedure. D,L-lactide (DLLA) and HPAE-OHs4 were dehydrated by using P_2O_5 under vacuum at 45°C for 24 h and were used without further purification. HPAE-OHs4 was put into a glass ampoule with predetermined amounts of D,L-lactide. $(Sn(Oct)_2)$ was added at about 0.1 (w/w) %. The ampoule was evacuated by a vacuum pump at 30°C for 1 h and then sealed. The ampoule was heated in an oil bath at 140°C for 13 h. After 13 h, the reaction product was cooled to ambient temperature. The obtained viscous material was dissolved with CH_2Cl_2 and then precipitated with petroleum, and washed further by petroleum for three times to remove unreacted DL-lactide monomers. After the petroleum was evaporated, the

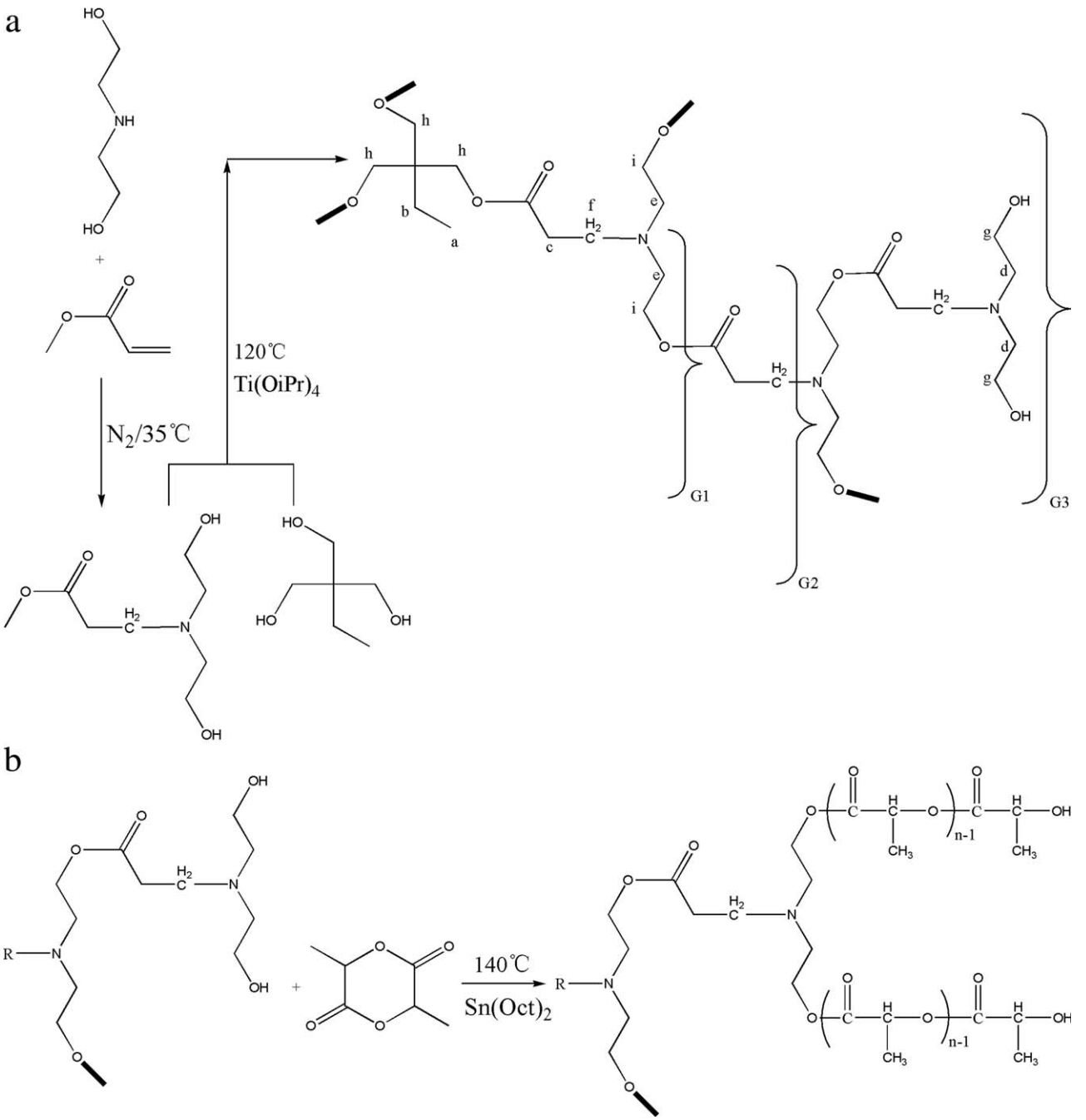

Scheme 1 (a) The synthesis route of HPAE-OHs; (b) The synthesis route of HPAE-*co*-PLA.

polymers were dissolved in a little of acetone and then precipitated in deionized water. The purified polymers were dried at 25°C for 2 days in a vacuum oven. The M_w of the PLA segement in the copolymers was controlled by the molar feed ratio of the monomer D,L-lactide. The polymerization route was shown in Scheme 1(b). The solubility of HPAE-*co*-PLA was totally opposite to HPAE-OHs4, which could be solved in acetone, dichloromethane and tetrahydrofuran (THF). It indicated that PLA was conjugated to the HPAE-OHs4. The different samples named HPAE-*co*-PLA 3 : 1 (feed ratio of D,L-lactide with HPAE-OHs4), HPAE-*co*-PLA 7 : 1 and HPAE-*co*-PLA 10 : 1, respectively, were synthesized.

Preparation of PLA

PLA and PLA nanoparticles were used to compare with HPAE-*co*-PLA copolymer and HPAE-*co*-PLA copolymer nanoparticles. PLA was prepared at 125°C for 10 h by the ring opening polymerization of D,L-lactide sealed in an ampoule in the presence of $Sn(Oct)_2$ as described previously.[23] The product was purified by the repeat dissolution in chloroform

and precipitation in cold methanol and was finally dried for 48 h at 40°C in a vacuum oven. The molecular weights were measured by gel permeation chromatography (GPC).

Determined the hydroxyl values of HPAE-OHs

The hydroxyl values of HPAE-OHs were determined by the following method.[24] HPAE-OHs was dissolved in excess benzoic anhydride with imidazole as a catalyst (in pyridine) at 80°C of water bath for 3 hours to acetylate the hydroxyl groups in HPAE-OHs. By back-titrating the above mixture with NaOH solution (0.1 mol L^{-1}, in water) at room temperature, the hydroxyl values of HPAE-OHs were calculated.

Determination of the chemical structure of HPAE–OHs and HPAE-*co*-PLA copolymer

FTIR spectra of HPAE–OHs and HPAE-*co*-PLA was obtained using a (Spectrum One, Perkin–Elmer) spectrophotometer. The spectra of HPAE–OHs were obtained by using KBr film as a reference. The HPAE-*co*-PLA samples were mixed with KBr and then pressed to a plate for measurement.

The ^{1}H-NMR spectra of HPAE-OHs and HPAE-*co*-PLA was recorded on a (Bruker AVANCE 400) NMR spectrometer. ^{1}H-NMR HPAE-OHs was dissolved in $(CD_3)_2SO$. HPAE-*co*-PLA copolymers were dissolved in $CDCl_3$.

The ^{13}C-NMR spectra of HPAE-OHs and HPAE-*co*-PLA was recorded on a (Bruker AVANCE 400) NMR spectrometer. ^{13}C-NMR HPAE-OHs was dissolved in $(CD_3)_2SO$. HPAE-*co*-PLA copolymers were dissolved in $CDCl_3$.

Gel permeation chromatography (GPC) was performed on a Waters 2410 GPC apparatus. Molecular weight and molecular weight distribution of the copolymer were calculated using polystyrene as the standard.

The thermal stability of HPAE-*co*-PLA and PLA samples were measured by TGA (Perkin–Elmer). The temperature range was from 25°C to 500°C under nitrogen flow and the heating rate was 20°C/min.

Preparation of HPAE-*co*-PLA copolymer nanoparticles

Double emulsion (DE) and nanoprecipitation (NP) methods were used to fabricate nanoparticles (NPs).[25,26]

The double emulsion (DE) method was used to fabricate nanoparticles as described by Rodrigues et al.[25] with a few modifications. Briefly, 0.20–2.0 mL BSA solution with 2–20 mg/mL concentration (in water) was emulsified in 1–5 mL of dichloromethane (DCM) containing HPAE-*co*-PLA (20–100 mg) by homogenization at 5000 rpm in an ice bath for 30s (Bailing, Model DS-200, China). Thereafter, this first emulsion was poured into 5–50 mL of the PVA aqueous solution (0.3–5%, w/v) and homogenized at 10,000 rpm in an ice bath for 45s (Bailing Model DS-200, China). The double emulsion (w/o/w) was diluted in 100 mL PVA solution (0.3%, w/v) and the DCM was rapidly eliminated by evaporation under reduced pressure. Finally, the nanoparticles were collected by centrifugation at 25,000 $\times$ g for 25 min at 4°C (Beckman Model J2–21) and washed twice with water. The nanoparticles were diluted with 2 mL of 5% glucose and stored at 4°C.

A nanoprecipitation (NP) technique[26] was developed for comparison with the DE method. Briefly, 1–5 mL of the polymer solution (10–100 mg/mL) in acetone was added dropwise to 1–20 mL of water with BSA (1–100 mg/mL) or without BSA at a rate of 0.5 mL/min using a syringe pump (74,900 series multichannel syringe pumps, Cole-Parmer Instrument Company) under magnetic stirring. Acetone was eliminated by evaporation under reduced pressure. The nanoparticles were recovered by ultracentrifugation and treated as above in the DE method.

The effects of copolymer composition and the preparation conditions, such as BSA concentration in water phase and copolymer concentration in organic phase, on the particle size and encapsulation efficiency (EE) were discussed.

Characterizations of the HPAE-*co*-PLA copolymer NPs

DSC measurement of NPs

The thermo-properties of the NPs with or without BSA, from the NP method, were investigated, and HPAE-*co*-PLA 7 : 1 (molar ratio) and PLA were taken as an example. Samples (3–5 mg) were loaded into aluminum pans and the DSC thermo grams were recorded on a Pyris Diamond DSC apparatus (Perkin–Elmer). To observe clear Tg, all of the DSC thermo grams were obtained from a second heating procedure. Briefly, the heating rate was 20°C/min in the range of 20–100°C by using nitrogen flowing, samples were stored at 100°C for 1 min and then cooled to −50°C, the cooling rate was 20°C/min, then the samples were reheated from 0 to 100°C in the heating rate of 20°C/min.

TEM observation

The morphological examination of nanoparticles was performed using a transmission electron microscope (TEM, JEM-200CX) following negative staining with sodium phosphotung state solution (2%, w/w).

TABLE I
The Hydroxyl Values of Different Generation HPAE-OHs[a]

Hydroxyl values of different generation HPAE-OHs	G2	G3	G4
Theoretical value (mgNaOH/g)	306	276	263
Experimental value (mgNaOH/g)	322	250	273

[a] G represent the generation of HPAE-OHs.

Measurements of particle size and ζ potential

Nanoparticle sizes and ζ potential were determined using a Zetasizer Nano series ZEN 3600 (Malvern Instruments, England). The experiment was performed at a wavelength of 633 nm with a constant angle of 90° at 25°C using the samples appropriately diluted with distilled water. For ζ potential, the sample was diluted with a 0.05 *M* NaCl solution to a constant ionic strength.

Measurements of EE

The encapsulation efficiency (EE) was determined by measuring the BSA concentration in the supernatant. The amount of nonentrapped BSA in aqueous phase was determined by the BCA protein assay in the supernatant obtained after ultracentrifugation of nanoparticles. The UV–visible spectroscopy measurements were carried out for known concentrations of BSA by using the BCA protein assay kit at the absorbance maximum of 562 nm. The EE was calculated as following equation:

$$\mathrm{EE}\ \% = 100\%(\mathrm{W_o} - \mathrm{W_t})/\mathrm{W_o}$$

W_o and W_t are the weight of initial BSA and that of the total amount of protein detected in supernatant after the twice centrifugation, respectively. Each sample was assayed in triplicate.

In vitro release

The NPs loading BSA were incubated in a capped centrifugal tube containing 8 mL of PBS (phosphate-buffered saline, pH 7.4), and the centrifugal tube was kept at 37°C water bath and shaken at 120 rpm. At appropriate intervals, 1 mL of the supernatant was extracted and equal amount of fresh PBS was added to the tube, the samples were centrifuged at 13,000 rpm for 10 min. BSA concentration in the supernatant was determined as described in above. Each experiment was repeated thrice and the result was the mean value of three samples. The error bars in the plot showed the standard deviation of data.

Stability of BSA released from NPs

The free BSA in the supernatant after its release of 14 days from the nanoparticles was stored at −20°C.

The secondary structure of released BSA and BSA control was determined by measuring circular dichroism spectra. The secondary structure was studied by CD spectra which was taken with a (Jasco J810) automatic recording spectropolarimeter at 25°C and 1 cm path length from 200 to 300 nm under nitrogen flow. Scan rates of 500 nm/min was used with a response time of 4 sec. The CD response obtained was expressed in terms of ellipticity.

The fluorescence spectra was further used to determine the tertiary structure of BSA released from NPs. Excitation was carried out at 285 nm, and emission spectra were recorded ranging from 300 to 440 nm. The excitation and emission bandwidths were 3 nm.

RESULTS AND DISCUSSION

Synthesis and characterization of HPAE–OHs and HPAE-*co*-PLA

Chemical structure of HPAE–OHs and HPAE-*co*-PLA

The hydroxyl values of different generation HPAE-OHs were measured and calculated by the method described in the previous article.[24] The results of different generation HPAE-OHs were showed in the Table I. It could be clearly seen that with the increase of generation the hydroxyl values were close to theoretical value, which indicated that the structure was apt to regulation.

The molecular weights and polydispersity indexes of the HPAE-*co*-PLA copolymers were shown in Table II.

TABLE II
Composition and Molecular Weight Distribution of HPAE-*co*-PLA Copolymers[a]

Sample	Copolymer	Molecular weight of copolymer		Polydispersity (M_w/M_n)
		M_w(kDa)	M_n(kDa)	
1	HPAE-*co*-PLA (3 : 1)	26	19	1.37
2	HPAE-*co*-PLA (7 : 1)	51	33	1.54
3	HPAE-*co*-PLA (10 : 1)	87	72	1.21

[a] M_w and M_n were measured by GPC.

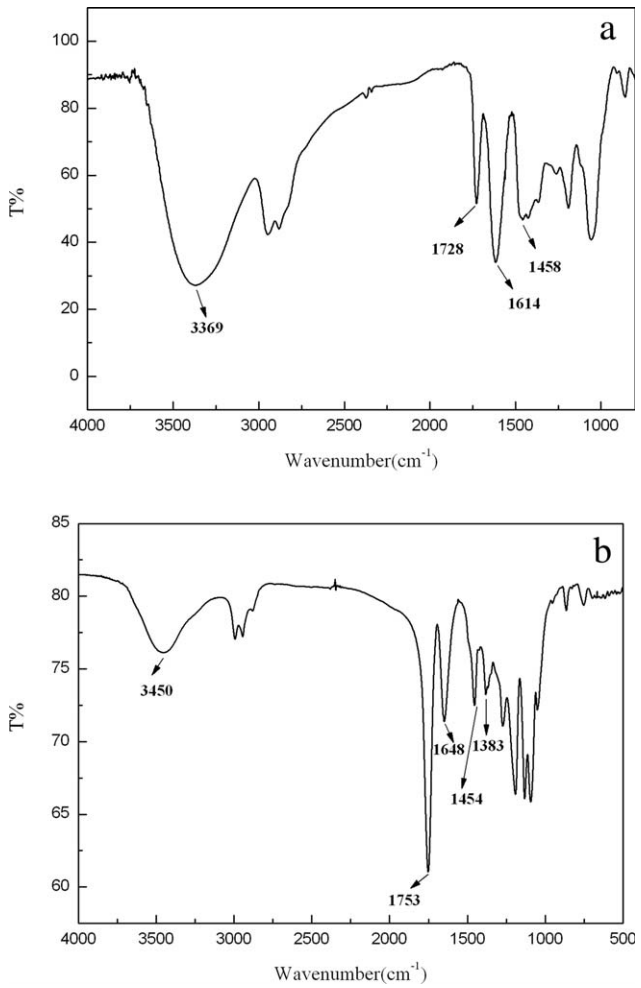

Figure 1 IR spectra of HPAE-OHs4 (a) and HPAE-*co*-PLA (3 : 1) (b).

The amount of lactide introduced to HPAE-OH4 increase with the molar ratio of DL-lactide to HPAE-OH4. When the molar ratio of lactide to HPAE-OH4 increased from 3 : 1 to 10 : 1, the molecular weights rose from 26 to 87 kDa. This indicated that the higher the concentration of lactide, the higher the opportunity for the lactide to react with HPAE-OH4 reactive centers.

Figure 1(a,b) showed the infrared spectra of the HPAE-OHs4 and HPAE-*co*-PLA. The CH_2 scissoring and wagging modes at 1457, 1442, and 1365 cm^{-1} were different between the two graphs. For the fourth generation of HPAE-OHs4, the intensity of the three absorption bands was weak and almost equivalent. While in HPAE-*co*-PLA, the band located at 1454 and 1383 cm^{-1} become much stronger than the other band. The band at 1191 cm^{-1} was corresponding to the C—O stretching vibration in HPAE-OHs4 alone, while in HPAE-*co*-PLA the absorption intensity become stronger than HPAE-OHs4 alone. The absorption peak appearing around 1753 cm^{-1}, corresponding to the carbonyl group of the branched polylactide [Fig. 1(b)] and the absorption peak around 1727 cm^{-1}, corresponding to the carbonyl group of HPAE-OHs4. All of these changes indicated the conformational change of the HPAE-OHs4 after the conjugation to the PLA, suggesting the hydrophilic and hydrophobic interaction between HPAE-OHs4 and PLA.

The basic chemical structure of HPAE-OHs4 and HPAE-*co*-PLA was further confirmed by ^{1}H-NMR [Fig. 2(a,b)].

Compared with HPAE-OHs4, the ^{1}H-NMR spectra of the HPAE-*co*-PLA copolymer [Fig. 2(b)] showed that the signals at 4.3 and 5.2 ppm were assigned to the terminal the methenyl protons of the branched polylactide and repeat units of it in the chain, respectively. The signals at 1.4 and 1.5 ppm were attributed to the methyl protons of the polylactied moiety located at the terminal groups and the repeat units of it in the chain. All these results evidenced that the new hyperbranched copolymers contained polylactide chains.

The basic chemical structure of HPAE-OHs4 and HPAE-*co*-PLA were further confirmed by ^{13}C-NMR, and the spectra were shown in Figure 2(c) (HPAE-OHs4) and Figure 2(d) (HPAE-*co*-PLA). Compared with HPAE-OHs4, the^{13}C-NMR spectra of the HPAE-*co*-PLA copolymer showed that the peak at ~170 ppm was attributed to the C=O group carbon peak of polylactide. The signals at 68 and 70 ppm were assigned to CH group carbon peak of the polylactide moiety located at the terminal groups and the repeat units of it in the chain. The signals at 17 and 20 ppm were attributed to the CH_3 group carbon peak of the polylactide moiety located at the repeat units and the terminal groups. All these results evidenced that the hyperbranched copolymer contained polylactide side chains.

TGA and DSC measurement

The thermal properties of HPAE-OHs4 and HPAE-*co*-PLA copolymers were examined by TGA measurement. Figure 3(a) showed TGA graphs observed for HPAE-OHs4, HPAE-*co*-PLA and PLA samples. Compared to HPAE-OHs4, HPAE-*co*-PLA copolymers have lower themal degradation temperature. A fast process of weight loss appears in the TG curves response for the PLA and HPAE-*co*-PLA copolymers in thermal degradation ranges. It could be seen that all of the copolymer samples exhibited a weight loss during the heating process, and the maximal weight loss rate temperature was about 210°C for all copolymer samples. The thermo decomposed rate and carbolic survivor increased with increase of the ratio of PLA in the copolymers. These results showed some decrease of the thermal stability for HPAE-*co*-PLA

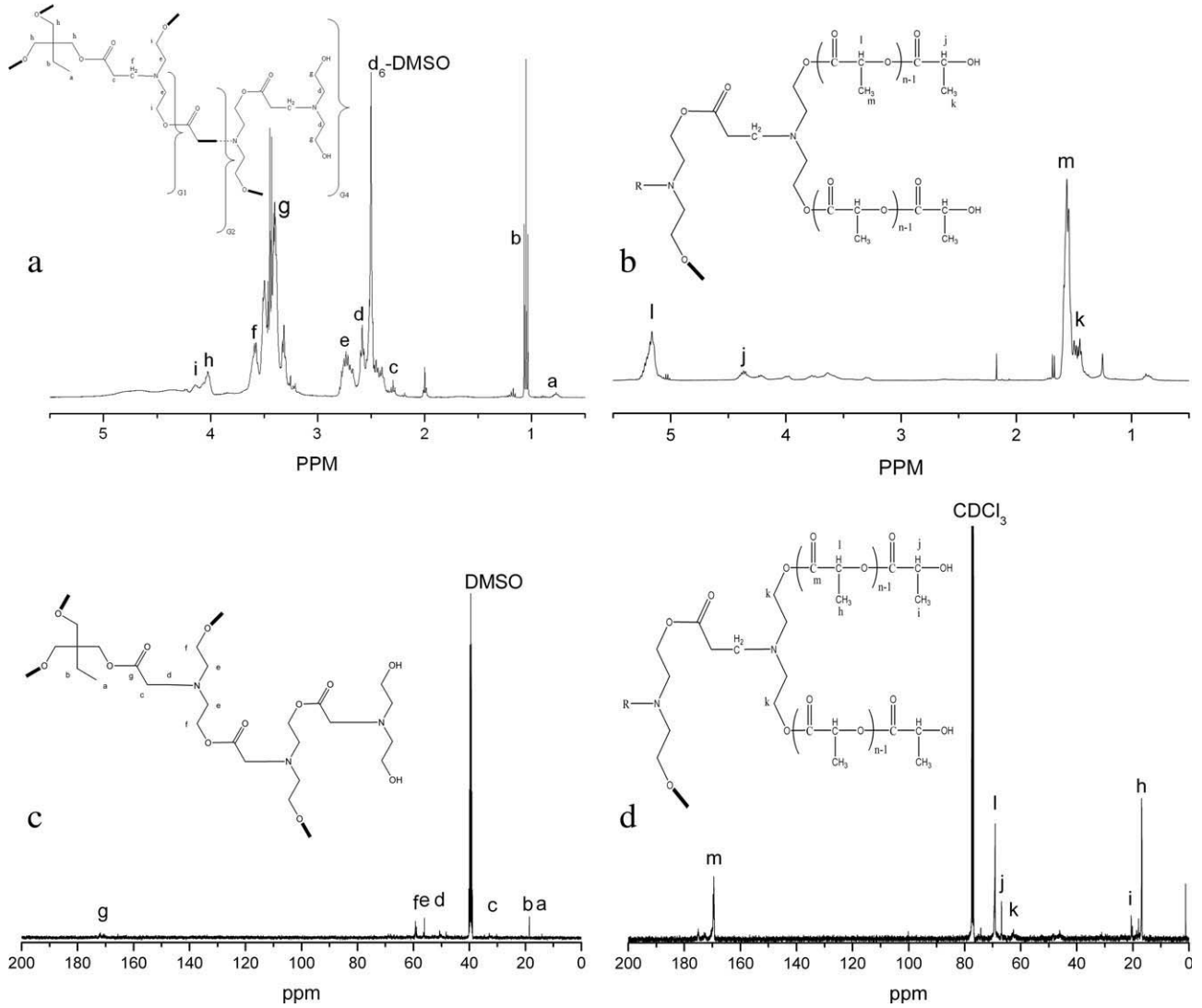

Figure 2 [1]HNMR spectrum of the HPAE-OHs4 (a), HPAE-*co*-PLA (b) and [13]CNMR spectrum of the HPAE-OHs4 (c), HPAE-*co*-PLA (d).

copolymer relative to the original HPAE-OHs4 and the thermal stability of the copolymer was decreased with increase of PLA segment.

To gain insight into the physical state of the copolymer and the NPs, The T_g of different samples were performed using DSC, and the results were shown in the Figure 3(b). Only one sidestep presented in all of the samples showed that there were no existence of inhomogeneities. 24.7°C could be used as the glass transition temperature of the HPAE-*co*-PLA which was far low compared to pure PLA after introduction PLA to HPAE-OHs4. The reason could be explained that HPAE-OHs4 with low T_g was elastic state at room temperature. The increase was observed in the T_g of blank NPs (T_g = 38.0°C) compared to HPAE-*co*-PLA. It could be explained that some micellization behaviors of the hydrophobic and hydrophilic interaction did existed after fabrication, which influenced the three dimension structure of copolymers and made the T_g increased. Compared blank NPs and BSA loaded NPs (T_g= 38.4°C), it showed that T_gs were almost the same. These results indicated that BSA had no obvious effect on the T_g during the fabrication process. The thermo properties of the NPs made by DE method were not shown here because PVA was used for stabilization and could not be washed entirely, the system was complicated for analyze.

Preparation of BSA loaded copolymer NPs

Effect of copolymer composition on particle size and EE

The copolymer composition has effect on the particle size of NPs. The higher M_w of PLA could lead to the high viscosity of copolymer solution and the decrease of HPAE-OHs4 relative contents, both

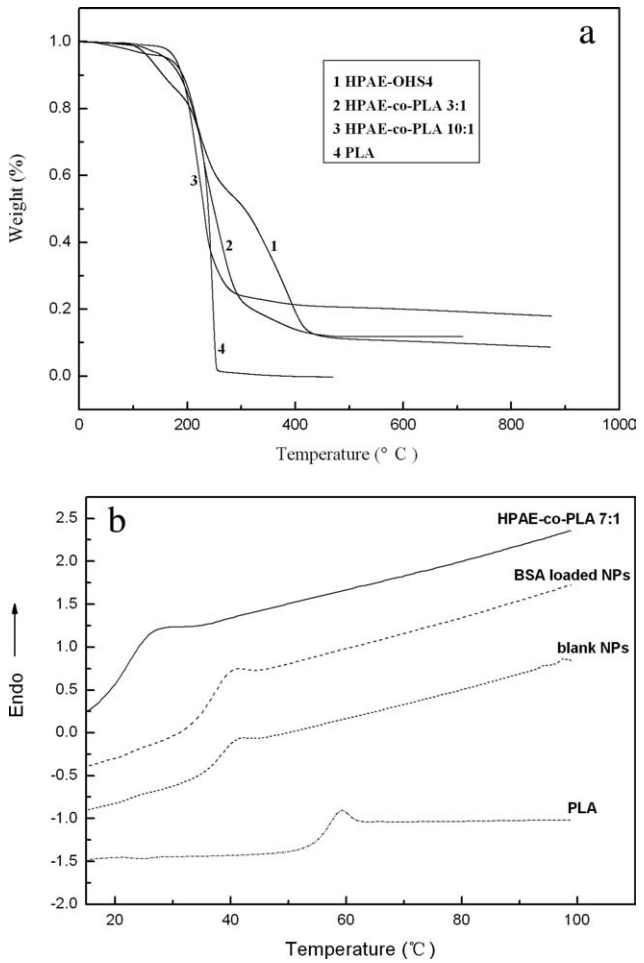

Figure 3 TGA graphs of HPAE-OHs4, HPAE-*co*-PLA3:1, 10:1 and PLA (M_w = 48 kDa) (a) and DSC (b) thermo grams of bulk matrix, frozen blank and BSA-loaded NPs made by NP method.

factors resulted in particle size increase. The increased viscosity could decrease the diffuse of BSA, which was in favor of EE enhancing, but on the other hand, the interactions between HPAE-OHs4 and BSA may decrease with the lowering of HPAE-OHs4 relative contents, which was unfavorable for enhancing EE. It meant that the copolymer composition impacted greatly on EE, especially when the HPAE-OHs4 relative contents decreased. For above reasons, the EE of different samples increased with the increasing of M_w of PLA when the feed ratio of PLA was added from 3 : 1 to 7 : 1, but as shown in the Table III, EE was declined when the HPAE-OHs4 relative contents were decreased to 10 : 1 (DLLA/ HPAE-OHs4). The encapsulation efficiency (EE%) of BSA in the HPAE-*co*-PLA nanoparticles was much improved in the comparision with EE% of BSA in the corresponding PLA nanoparticles. The reasons for high EE% will be considered as follows. Firstly, Hyperbranched polymers have unique chain structure. Distinct from their linear analogs, hyperbranched polymers have structures and topologies similar to those of dendrimers, and possess some strikingly superior material properties, such as low solution/melt viscosity, enhanced solubility, abundance in terminal group, etc. Hyperbranched polymers contain numerous end-groups in their molecular structures and the characteristics of these terminal groups have a great influence on the properties of resulting hyperbranched polymers. The hyperbranched moiety was favorable for interactions between HPAE-OHs4 and BSA. Secondly, the copolymer HPAE-*co*-PLA was amphiphilic so that its hydrophilic part was accessible to the water-soluble BSA molecule. All the effects contributed to the increased EE%. If the HPAE-OHs moiety was helpful for the improvement of EE%, it was easy to understand why the HPAE-*co*-PLA copolymer could form the nanoparticles loading more BSA. Of course, the better hydrophilic/ hydrophoblic balance of the HPAE-*co*-PLA copolymer must be important.

TABLE III
Effect of Material Composition on EE and Particle Size[a,b,c,d]

Method	Material composition	EE (%)	Mean hydrodynamic diameter (nm)	PDI	Zeta potential (mv)
DE	3 : 1 (HPAE-*co*-PLA)	62.80 ± 2.1	142.9 ± 1.1	0.296–0.315	−13.6 ± 1.2
DE	7 : 1 (HPAE-*co*-PLA)	81.30 ± 0.6	149.4 ± 2.2	0.177–0.197	−22.5 ± 1.4
DE	10 : 1 (HPAE-*co*-PLA)	51.00 ± 1.3	163.4 ± 3.8	0.129–0.231	−26.5 ± 2.3
NP	3 : 1 (HPAE-*co*-PLA)	18.60 ± 3.2	142.3 ± 0.9	0.124–0.166	−21.3 ± 0.6
NP	7 : 1 (HPAE-*co*-PLA)	59.80 ± 2.6	146.8 ± 1.6	0.087–0.133	−22.3 ± 1.4
NP	10 : 1 (HPAE-*co*-PLA)	36.02 ± 0.6	163.2 ± 4.3	0.120–0.145	−30.6 ± 1.9
DE	PLA	43.56 ± 2.2	410.2 ± 4.6	0.152–0.224	−32.25 ± 2.5
NP	PLA	33.67 ± 3.1	251.8 ± 5.4	0.206–0.246	−43.16 ± 1.1

[a] For DE method, 0.5 mL BSA solution (10 mg/mL) was used as inner aqueous phase. 50 mg copolymer HPAE-*co*-PLA was dissolved in 2.5 mL dichloromethane, 50 mg PLA was dissolved in 3 mL dichloromethane/acetone (1 : 1), PVA concentration was 3% (w/v).

[b] For NP method, 5 mg BSA was dissolved in 10 mL water, 50 mg copolymer was dissolved in 1 mL acetone, 50 mg PLA was dissolved in a mixture consisting of 1 mL acetone and 0.05 mL dichloromethane.

[c] Molecular weight (M_w = 48 kDa) of PLA homopolymer was similar to the molecular weight of PLA in copolymer of HPAE-*co*-PLA (7 : 1).

[d] PDI represents polydispersity index.

TABLE IV
The Influence of Fabricating Factors on EE and Particle Size by DE Method[a,b]

BSA Con. (g/mL)	Internal phase volume(mL)	Polymer weight (mg)	PVA Con. (w/v %)	EE (%)	Mean diameter (nm)	PDI	Zeta potential (mv)
0.005	0.50	50	3	38.4 ± 2.3	161.1 ± 4.1	0.167–0.212	−23.9 ± 1.0
0.010	0.50	50	3	81.3 ± 0.6	149.4 ± 2.2	0.177–0.197	−22.5 ± 1.4
0.015	0.50	50	3	52.3 ± 1.3	141.6 ± 3.0	0.204–0.230	−29.0 ± 0.8
0.010	1.00	50	3	55.5 ± 1.0	145.1 ± 4.3	0.134–0.186	−33.9 ± 1.0
0.010	0.25	50	3	31.8 ± 1.5	163.7 ± 3.6	0.083–0.149	−32.7 ± 0.7
0.010	0.50	25	3	60.4 ± 2.7	132.6 ± 3.9	0.084–0.120	−55.9 ± 2.1
0.010	0.50	75	3	96.6 ± 0.3	152.1 ± 2.7	0.177–0.231	−31.0 ± 1.4
0.010	0.50	50	1	73.6 ± 2.3	167.8 ± 4.5	0.123–0.225	−32.8 ± 1.1
0.010	0.50	50	4	97.8 ± 0.4	150.2 ± 5.0	0.109–0.155	−21.0 ± 1.2

[a] HPAE-*co*-PLA7:1 was used as an example.
[b] Con. represents concentration, and PDI represents polydispersity index.

Effect of fabrication method on particle size and EE

DE technique

DE method was chosen as the most appropriate method because protein is highly soluble in water. The result was shown in Table IV.

Effect of BSA concentration in the inner aqueous phase on particle size and EE

It was reported that BSA tend to accumulate at air/water, oil/water or solid/water interfaces. Therefore, the BSA could act as an excellent surfactant which was widely used to stabilize emulsions and further influence the particle size.[27]It meant that with the increase of the protein concentration in the inner aqueous phase, the particle size became smaller. EE increased at first with higher protein concentration in the inner aqueous phase. EE decreased a lot when protein concentration in the inner aqueous phase was increased from 0.01 to 0.015 g/mL. The difference in osmotic pressure between the internal and external aqueous phases could be responsible for the decrease in entrapment efficiency. The osmotic pressure difference did rise with increase of BSA loading and promote an exchange between the internal and external aqueous phases, with a consequent loss of BSA.[28]

Effect of inner aqueous phase volume on particle size and EE

Coalescence of droplets could be prevented by increasing internal phase. An increase in the internal aqueous phase volume of the same concentration led to a decrease of nanoparticles' average size. Since an opposite effect exists, EE showed same phenomena as mentioned in the above section. It was reported that the precipitation of the polymer solution phase was accelerated and the hardening time was shortened with the increase of inner aqueous, which was in favor of EE.[27]As mentioned in the above section, when the content of BSA was increased at a certain extent, BSA was lost from inner phase to outer phase.

Effect of polymer concentration in organic phase on particle size and EE

Since a high viscosity hampered the shear forces of emulsion, an increase in the polymer concentration resulted in an increase of the particle mean diameter from 132.6 to 152.1 nm with a broadened particle size distribution. While the EE increased when the polymer concentration in organic phase increased since high viscosity and more HPAE-OHs4 relative contents avoided the loss of BSA.

Effect of PVA concentration in external aqueous phase on particle size and EE

PVA is an emulsifier. The concentration of PVA had a significant effect on the formulation of nanoparticles in DE method. An increase in external aqueous concentration of PVA from 1 to 4% (w/v) led to a decrease in particle size. As PVA concentration higher than 3%, the decrease in NP size was very small. The similar result was reported by previous article.[29] BSA EE% was increasing with the increase of the concentration of PVA. The reason was that tight surface was formed from PVA macromolecules of high concentration, which increased diffusion resistance of BSA from the internal aqueous phase and stabilized the emulsion. But too much PVA which could not be entirely biodegraded *in vivo* was difficult to remove.

NP method

NP method was a relative mild technique as compared with DE method because sonicators were not used by NP method. This technique also allowed for the preparation of large quantities of NPs since sonicators and homogenizers were not used in the process.[30] Briefly, NP technique was to precipitate the NPs through the use of an organic solvent that was

TABLE V
The Influence of Fabricating Factors on EE and Particle Size by NP Method[a,b]

No.	BSA conc. (mg/mL)	Polymer weight (mg)	EE (%)	Mean diameter (nm)	PDI	Zeta potential (mv)
1	0.25	50	28.1 ± 1.5	152.9 ± 2.5	0.049–0.114	−30.5 ± 2.3
2	0.5	50	59.8 ± 2.6	146.8 ± 1.6	0.087–0.133	−22.3 ± 1.4
3	0.75	50	55.7 ± 1.0	120.9 ± 3.3	0.087–0.124	−20.3 ± 1.6
4	0.5	25	53.8 ± 1.3	158.1 ± 4.5	0.117–0.220	−19.2 ± 0.89
5	0.5	75	61.4 ± 1.0	173.4 ± 3.4	0.096–0.156	−24.3 ± 1.2

[a] HPAE-*co*-PLA7:1 was used as an example.
[b] Con. represents concentration, and PDI represents polydispersity index.

entirely miscible with water. The formation of NPs with NP method could be carried out without any surfactant due to the amphiphilic properties of copolymers. Both the particle size and EE increase with the increase of copolymer concentration in acetone. While the EE increased first and then decreased with the increase of BSA concentration. These could be explained as mentioned in above sections. The particular results were listed in Table V.

The above data showed that the fabrication method had a significant effect on the EE. NPs with EE of 31.8–97.8% could be prepared by using DE method. Meanwhile, NPs with EE of 28.1–61.4% could be fabricated by using NP method at various conditions. The structure of HPAE-OHs4 hyperbranched moiety might be in favor of EE enhancement.

The structure preservation of BSA was also considered during its nanoencapsulation. Blending acetone in the organic phase with methylene chloride probably limited the contact between methylene chloride and BSA as well as reduced the surface tension between the organic phase and the water. The presence of acetone allowed NPs to solidify as a result of its solubility into water.[31] In addition, proteins are heat-sensitive and sonication is an exothermic operation. Therefore, the ice bath was used during primary emulsion.

Other experimental technique should be paid attention to during encapsulation. A rotation evaporator was used to reduce the evaporation time to avoid the protein release during stirring at room temperature. Moreover, organic solvent must be evaporated completely since the remained organic solvent will cause caking during centrifugation.[32]

Morphology

The morphology of the NPs was investigated by the transmission electron microscopy technique. Figure 4 showed the TEM image of NPs. It could be confirmed that the NPs appeared to be fine spherical shapes and no aggregation or adhesion occurred among the NPs made by both NP and DE methods.

In vitro release of BSA

The release profiles of BSA from the HPAE-*co*-PLA nanoparticles comparing with PLA nanoparticles were investigated and displayed in Figure 5. The curve shape in the BSA release from the HPAE-*co*-PLA nanoparticles was similar as that from the PLA nanoparticles although the BSA release from HPAE-*co*-PLA nanoparticles was much faster. After the

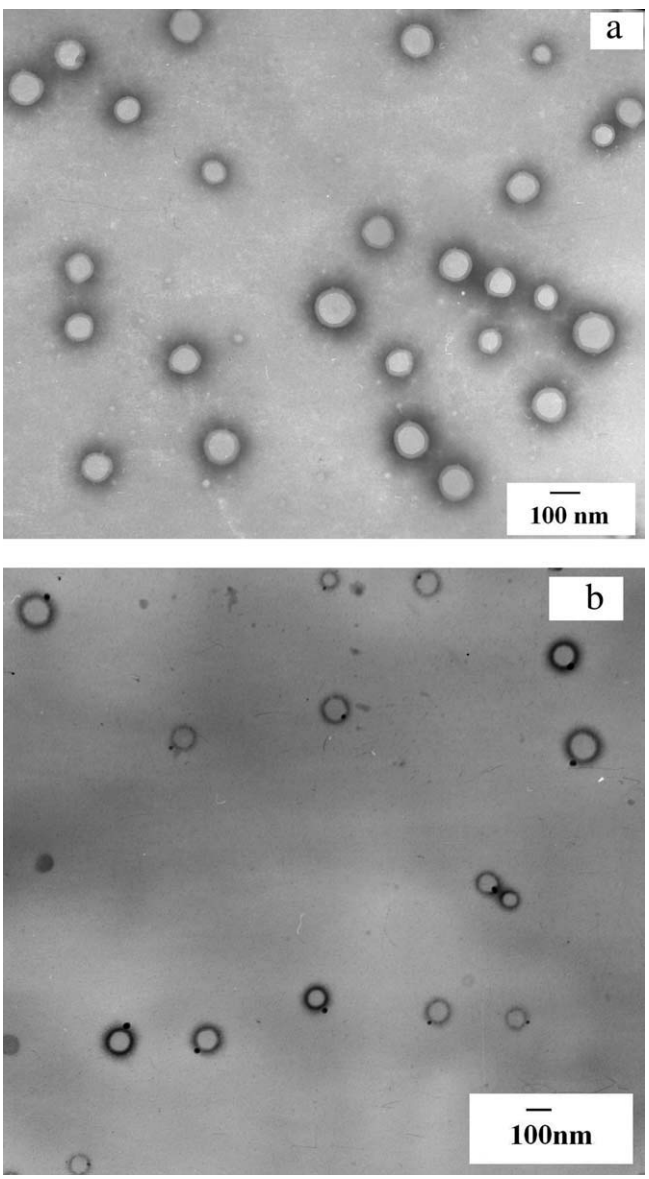

Figure 4 TEM images of BSA-loaded HPAE-*co*-PLA NPs fabricated by DE (a) and NP (b).

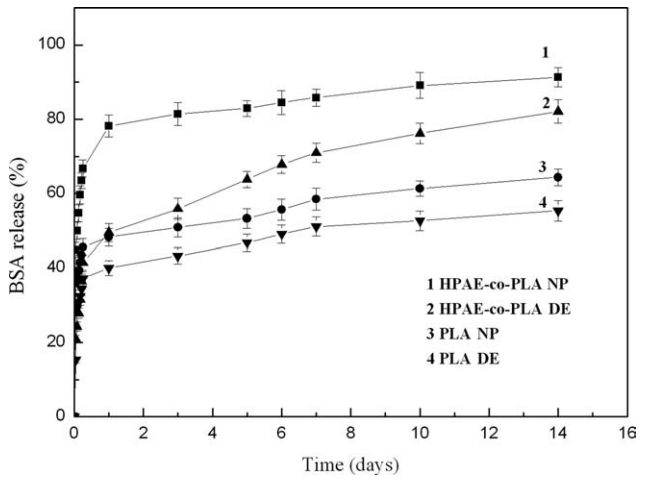

Figure 5 *In vitro* release profiles of BSA from the PLA (M_w = 48 kDa) and HPAE-*co*-PLA (7 : 1) nanoparticles.

initial burst, BSA release profiles displayed a sustained fashion. This sustained release could result from diffusion of BSA into the polymer wall and the protein through polymer wall as well as the erosion of the polymers. In this article, a higher and faster BSA release was observed for HPAE-*co*-PLA nanoparticles than those of PLA. The difference could be relation to the presence of HPAE-OHs in PLA chains. There could be more protein molecules close to HPAE-*co*-PLA nanoparticles surface including those inserted among HPAE-OHs hyperbranched moiety on the surface of nanoparticles, which also would be much faster released. In all of the curves a burst effect was observed and a slow continuous release phase was followed. The maximal released amount is 82.13% for DE method and 91.28% for NP method in HPAE-*co*-PLA nanoparticles, respectively.

It was noticed that different fabrication methods led to various release behavior. The released amount and rate of BSA from NPs with NP method was much faster than that of DE method. The same result was also showed as previously reported.[33] When the polymers are not soluble in water, drug molecules dissolved in water may be very close to the outer NPs surface, forming a layer of molecules, susceptible to be easily and rapidly released. In addition, more burst release was observed from NPs fabricated with NP technique than those from DE method. This was because different methods led to various distributions of BSA molecules in the NPs. The fabrication method determined the amount of protein existing near the surface of NPs. Using DE method, most BSA molecules were encapsulated within the NPs as the multinanoreservoir systems. Using NP method, NPs were formed as the multimolecular polymeric micelles trapping BSA molecules near their outer layers.

Stability of BSA released from NPs

Circular dichroism spectroscopy is a common method to analyze the secondary structure of a protein with high reliability. In the CD spectrum of the native BSA in PBS (pH 7.4), there were two extreme valleys at 208 and 222 nm.[34] The CD spectra of the free BSA in the supernatant from the release test after 14 days was measured and shown in Figure 6(a). Obviously, two extreme valleys at 208 and 222 nm occurred without any significant difference from those of the native BSA. The result indicated that the released BSA remained its original structure. The intensities of the double minimums reflected the helicity of BSA as more than 50% of α-helical structure. The declined intensity of the double minimums implied that the extent of α-helicity of the protein decreased. Because NP method fabricated nanoparticles in a more mild way, as for the HPAE-*co*-PLA nanoparticles, the secondary structure of the released BSA from the nanoparticles fabricated by the NP method remained more stable than by DE method. Compared to the CD spectrum of native

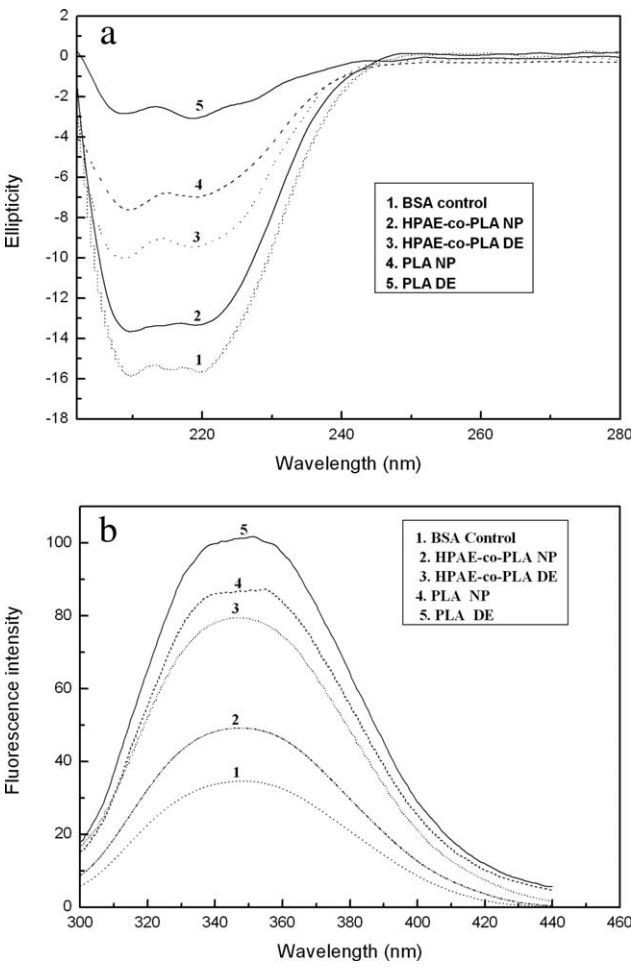

Figure 6 The CD spectra (a) and the fluorescence spectra (b) of BSA released 14 days from NPs fabricated by DE and NP methods [HPAE-*co*-PLA (7 : 1), PLA (M_w = 48 kDa)].

BSA, the CD spectrum of the supernatant BSA released from the HPAE-*co*-PLA nanoparticles conformed more than that of BSA released from the PLA nanoparticles, indicating that the secondary structure of BSA released from HPAE-*co*-PLA nanoparticles was kept more stable than that from the PLA nanoparticles. The HPAE-*co*-PLA nanoparticles of a protein might be promising as a nasal delivery system, because the biological response of proteins encapsulated in some biodegradable nanoparticles was significantly greater than those in the microparticles when administered intranasally.

Meanwhile, fluorescence spectrum has been further used as a sensitive detector for the conformational change studies in the tertiary structures,[35] as shown in Figure 6(b). The fluorescence emission spectrum of BSA at an excitation of 285 nm showed at 349 nm. Likewise, tertiary structure of BSA was also similar to BSA controlled.

CONCLUSIONS

A series of biodegradable block copolymers of HPAE-*co*-PLA were synthesized. FTIR, ^{1}H-NMR, ^{13}C-NMR, TGA, and DSC were used to investigate the physico–chemical characteristics of the hyperbranched copolymer. Conjugating of PLA to HPAE-OHs was proved to be an available method for the preparation of NPs for protein delivery. The BSA loaded NPs fabricated by DE and NP methods were proved having following properties: the bio-application of hyperbranched copolymer nanoparticles, the enhancement of EE and the structural stability of BSA during the released process. It was also shown that both copolymer composition and fabrication methods have obviously effect on particle size, EE and release process. All above researches helped to recognize and design a new route of delivery system.

References

1. Leo, E.; Ruozi, B.; Tosi, G.; Vandelli, M. A. Int J Pharm 2006, 323, 131.
2. Mouffouk, F.; Chishti, Y.; Jin, Q.; Rosa, M. E.; Rivera, M.; Dasa, S.; Chen, L. H. Anal Biochem 2008, 372, 140.
3. Liu, M.; Zhou, Z. M.; Wang, X. F.; Xu, J.; Yang, K.; Cui, Q.; Chen, X.; Cao, M. Y.; Weng, J.; Zhang, Q. Q. Polymer 2007, 48, 5767.
4. Yang, L.; Zhao, Z. X.; Wei, J.; Abdelslam, E. G.; Li, S. M. J Colloid Interface Sci 2007, 314, 470.
5. Dong, Y. C.; Feng, S. S. Biomaterials 2007, 28, 4154.
6. Choi, S. W.; Kim, J. H. J Controlled Release 2007, 122, 24.
7. Takami, A.; Masanori, B.; Mitsuru, A. Polymer 2007, 48, 6729.
8. Bikiaris, D. N.; Karayannidis, G. P. Polym Int 2003, 52, 1230.
9. Gao, C.; Yan, D. Prog Polym Sci 2004, 29, 183.
10. Mckee, M. G.; Unal, S.; Wilkes, G. L.; Long, T. E. Prog Polym Sci 2005, 30, 507.
11. Aulenta, F.; Hayes, W.; Rannard, S. Eur Polym J 2003, 39, 1741.
12. Shcharbin, D.; Mazur, J.; Szwedzka, M.; Wasiak, M.; Palecz, B.; Przybyszewska, M.; Zaborski, M.; Bryszewska, M. Colloids Surf B: Biointerfaces 2007, 58, 286.
13. Kaneko, Y.; Imai, Y.; Shirai, K.; Yamauchi, T.; Tsubokawa, N. Colloids Surf A: Physicochem Eng Aspects 2006, 289, 212.
14. Sha, Y. W.; Shen, L.; Hong, X. Y. Tetrahedron Lett 2002, 43, 9417.
15. Twyman, L. J.; King, A. S. H.; Burnett, J.; Martin, I. K. Tetrahedron Lett 2004, 45, 433.
16. Tian, H. Y.; Deng, C.; Lin, H.; Sun, J. R.; Deng, M. X.; Chen, X. S.; Jing, X. B. Biomaterials 2005, 26, 4209.
17. Rajesh, K. K.; Muthiah, G.; Munia, G.; Tanay, G.; Donald, E. B.; Souvik, M.; Jayachandran, N. K. Biomaterials 2006, 27, 5377.
18. Hyun, J. K.; Min, S. K.; Joon, S. C.; Bo, H. K.; Jae, K. Y.; Kwan, K.; Jong-Sang, P. Bioorg Med Chem 2007, 15, 1708.
19. Lu, Y.; Lin, D.; Wei, H. Y.; Shi, W. F. Acta Polym Sinica 2000, 4, 411.
20. Bao, C. Y.; Jin, M.; Lu, R.; Zhang, T. R.; Zhao, Y. Y. Mater Chem Phys 2003, 82, 812.
21. Quellec, P.; Gref, R.; Perrin, L.; Dellacherie, E.; Sommer, F.; Verbavatz, J. M.; Alonso, M. J. J Biomed Mater Res 1998, 42, 45.
22. Karayannidis, G. P.; Roupakias, C. P.; Bikiaris, D. N.; Achilias, D. S. Polymer 2003, 44, 931.
23. Hyon, S. H.; Jamshidi, K.; Ikada, Y. Biomaterials 1997, 18, 1503.
24. Zhu, B. K.; Wei, X. Z.; Xiao, L.; Xu, Y. Y.; Geckeler, K. E. Polym Int 2006, 55, 63.
25. Rodrigues, J. S.; Santos-Magalhaes, N. S.; Coelho, L. C. B. B.; Couvreur, P.; Ponchel, G.; Gref, R. J Controlled Release 2003, 92, 103.
26. Govender, T.; Stolnik, S.; Garnett, M. C.; Illum, L.; Davis, S. S. J Controlled Release 1999, 57, 171.
27. Verrecchia, T.; Spenlehauer, G.; Bazile, D. V.; Murry-Brelier, A.; Archimbaud, Y.; Veillard, M. J Controlled Release 1995, 36, 49.
28. Lamprecht, A.; Ubrich, N.; Hombreiro Pe'rez, M.; Lehr, C. M.; Hoffman, M.; Maincent, P. Int J Pharm 1999, 184, 97.
29. Ferdous, A. J.; Stembridge, N. Y.; Singh, M. J Controlled Release 1998, 50, 71.
30. Birnbaum, D. T.; Kosmala, J. D.; Brannon-Peppas, L. J Nanopart Res 2000, 2, 173.
31. Zambaux, M. F.; Bonneaux, F.; Gref, R.; Dellacherie, E.; Vigneron, C. Int J Pharm 2001, 212, 1.
32. Zambaux, M. F.; Bonneaux, F.; Gref, F.; Dellacherie, E.; Vigneron, C. J Biomed Mater Res 1999, 44, 109.
33. Ubrich, N.; Bouillot, P. H.; Pellerin, C.; Hoffman, M.; Maincent, P. H. J Controlled Release 2004, 97, 291.
34. Molina, I.; Li, S.; Martinez, M. B.; Vert, M. Biomaterials 2001, 22, 363.
35. Sułkowska, A.; Bojko, B.; Rownicka, J.; Sułkowski, W. Biopolymers 2004, 74, 256.